

# Sub-centimeter Probes for Low-Frequency Alternating Electric Field (AEF) Measurements in Rodent Models of Brain Cancer

Marinus H. Daling<sup>1</sup>, David Durfee<sup>1</sup>, Turner Shelton<sup>1</sup>, Samuel Simonian<sup>1</sup>,  
Keith Schubert<sup>1</sup>, Sabbir Khan<sup>2</sup>, Chirag B. Patel<sup>2</sup>, Vincent W. Leung<sup>1</sup>

<sup>1</sup>Baylor University, Waco, TX, USA

<sup>2</sup>The University of Texas MD Anderson Cancer Center, Houston TX, USA

**Abstract**— The FDA has approved therapeutic low frequency alternating electric fields (AEFs), called tumor treating fields (TTFields), for the treatment of patients with glioblastoma, malignant pleural mesothelioma, and non-small cell lung cancer. Accurate measurements of these fields in rodent models are critical for the pre-clinical development and testing of combinatorial therapeutic strategies involving AEF before they can be translated to human clinical trials. This paper presents a novel 3mm diameter electric field probe capable of measuring such fields. The probe demonstrates a measurable field range of 0.1 – 10  $V_{pp}/cm$  at 200  $kHz$ . The proposed probe significantly outperforms a commercially available stub probe with a measurement error of 18 % in a known field, compared to an error of 94.4 % for the commercial probe. Measurement of an applied AEF in a rat skull, with electrodes similar to those used in clinical trials, is also demonstrated with a maximum measurement error of  $\pm 5.5$  % between three different probes. This simple sensor is made from commercially available components and operates over a wide range of frequencies and field strengths, making it ideal for preclinical AEF validation and potentially transferable to future clinical applications.

**Keywords**—Electric Field Probe, Tumor Treating Fields, Alternating Electric Fields

## I. INTRODUCTION

Glioblastoma is the most common form of brain cancer in adults, and despite the standard therapies, the median overall survival is 16-20 months from diagnosis, with a dismal 5-year survival rate of 5.6%.

The FDA has approved therapeutic alternating electric fields (AEFs), called tumor treating fields (TTFields), for the treatment of patients with glioblastoma (200  $kHz$ ), malignant pleural mesothelioma (150  $kHz$ ), and non-small cell lung cancer (150  $kHz$ ). AEF intensity of 1  $V_{pp}/cm$  (peak-to-peak) has been shown to have anti-cancer efficacy [1]. Orthotopic rodent models of glioblastoma recapitulate the tumor biology well, thereby enabling clinically-relevant research of novel therapies.

Measurement of induced electric fields in tissue is necessary to ensure that the threshold therapeutic AEF intensity of 1  $V_{pp}/cm$  is successfully achieved. Additionally, measurements can account for inhomogeneities in rodent brains (i.e., gray matter, white matter, cerebrospinal fluid), which homogeneous phantoms used in in-silico models fail to do. While a sensor of this type is important to determine TTFields effects on tumors, there is also a great deal of interest in measurements for safety standards related to the human radiofrequency exposure. This is especially true for frequencies below 300  $kHz$  [2].

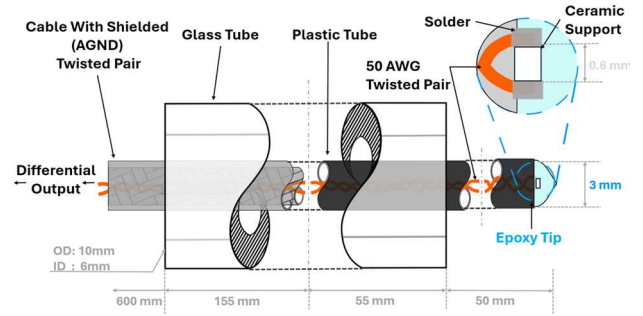


Figure 1. Design of proposed electric field probe.

These therapeutic and safety concerns create a need for appropriate probes that can verify that the threshold therapeutic field strength is achieved, and that the exposure does not exceed the maximum permissible exposure (MPE) [3]. The probe must be small enough to be introduced via a small burr hole ( $< 5$  mm) in the skull and be capable of measuring low frequency alternating fields without perturbing said fields.

MEMS-based piezoelectric sensors were recently proposed in [4], but their fabrication is complex and their sensitivity to gravitational forces can create distortion in some cases. Solid-state options such as field-effect transistors or varactors were also proposed [4], but active driving changes the field surrounding the sensor, making them unsuitable for clinical validation.

Small, efficient antennas are available for cell phone frequencies at hundreds of megahertz and higher [5], which are too high for TTFields research. On the other hand, antennas developed for the LF band (30 – 300  $kHz$ ), generally based on dipoles that are over 10 cm in length [6], are too big. While consumer-grade small-sized near-field LF probes are available, researchers should use caution as these commercial solutions may not provide satisfactory results, as will be demonstrated shortly.

The constraints of these technologies have directed efforts towards the design of small, low frequency probes based on tiny dipoles. The system proposed in [7] uses 200  $\mu m$  silver-silver chloride tipped wires spaced 20 mm apart to detect 60  $Hz$  fields in rat tissues. But insulated probes are preferred to prevent perturbation of the fields. To measure electric fields generated by high power switching electronics, which appear at frequencies similar to the TTFields, the systems of [8-9] employ printed circuit boards with parallel traces connecting

the dipoles to instrumentation amplifiers. Both appear to have electronics that are ground referenced.

This work proposes a 3 mm diameter electric field sensor based on an electrically short dipole antenna but does not refer to the earth ground. As a result, the probe exhibits good operation at the low frequencies of interest *without* perturbing the field, making it suitable for validating AEF field strength in pre-clinical studies.

The paper is organized as follows. Section II details the design of the electric field probe and amplification electronics. Section III shows the probe's response to electric fields and proposes its electromechanical behavior. Section IV presents the results of electric field measurements conducted within a rat skull. A Summary is given in Section V.

## II. PROBE DESIGN

### A. Design of the Electric Field Probe

Figs. 1 and 2(a) show the design of the proposed electric field probe. The separated ends of a 50 AWG enameled copper twisted wires, similar to a dipole antenna, are used as a sensing element. For precision dimension control and mechanical support, they are connected to the solder pads of the ceramic frame of a 0402 surface mount inductor (with the wire-wound inductor removed). The resulting probe tip is encased in a non-conductive polyepoxide to electrically isolate it (Fig. 2a), and the twisted pair is fed through a plastic tube with 3 mm diameter and 5 cm length. Once the twisted pair connection has left the vicinity of the sensor site, it is attached to a shielded twisted cable for improved interference rejection. The cable allows the amplification electronics to be located far from the sensing area. The plastic tube/shielded cable is encased by a glass tube of 1 cm outer diameter to improve probe rigidity and ease of handling. Fig. 2(b) shows a picture of the constructed probe.

The proposed probe does not use a ground shield as a means of noise reduction, as is done in some commercially available stub probes. By providing a low impedance path to the “earth” ground, a ground shield can perturb the field that the probe tries to measure. Rather, the twisted pair mentioned earlier provides noise reduction without perturbing the measured field. The small gauge twisted wires: (a) minimize the loop area affected by inductive coupling, (b) aid in passive cancellation of any ambient magnetic fields, and (c) provide measurement immunity to capacitive coupling by causing such noise to be common mode.

### B. Design of Amplification Electronics

Fig. 3 shows a block diagram of the sensor electronics, designed to amplify low-amplitude voltage signals picked up by the dipole, while maintaining isolation from the earth ground to minimize interfering with the electric field under evaluation. The first stage uses an instrumentation amplifier (IA) from Analog Devices (AD8421) to reject common mode

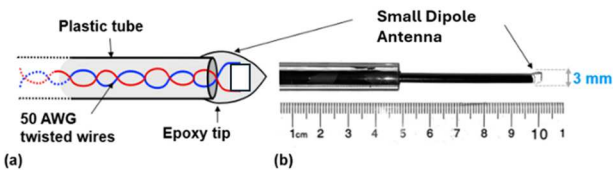


Figure 2. (a) Close up illustration of probe tip. (b) Picture of constructed probe

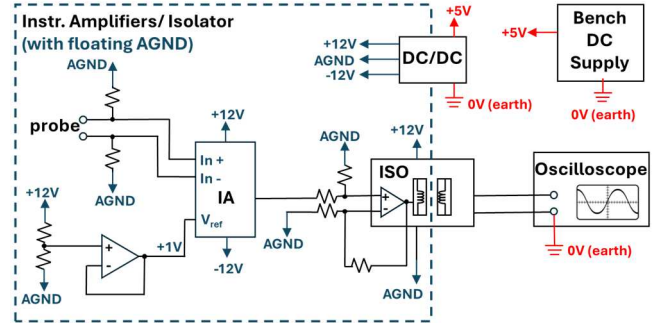


Figure 3. Block diagram of amplification electronics with isolated power domain indicated in blue.

noise and provide a gain of 100 V/V. The IA has a typical input impedance of 10 GΩ, a linear input voltage range of 0 – 25 mV, and a 3 dB cutoff frequency of 325 kHz.

To prevent the earth ground (0 V) from disturbing the field being measured by the probe, all amplifier electronics are isolated/biased by a commercial DC/DC converter from Traco (TMH 0512D), which supplies powers ( $\pm 12$  V) and a floating ground (AGND).

The IA output is coupled to the oscilloscope through an isolated error amplifier from Analog Devices (ADuM3190) with a gain of 2.6 V/V. To reject common-mode noise on the signal and AGND lines, it is set up as a difference amplifier with four 3 kΩ resistors with 0.5% tolerance. A 1 V reference voltage is supplied by a voltage buffer (formed by LM741 operational amplifier) to ensure the IA output voltage aligns with the isolator input range.

The overall gain of this isolated amplification system is 260 V/V. It was built using vendor evaluation boards with minor modifications. We anticipate that even greater isolation is possible if a small, custom printed circuit board, using the same components, were used.

## III. SENSOR CHARACTERIZATION

As shown in Fig. 4(a), two copper-clad FR4 boards ( $200 \times 150$  mm) are used to create a uniform electric field in which three probes (denoted A, B and C) will be evaluated. The boards are spaced 4 cm apart and connected to a differential sinusoidal drive. The bipolar AEF signal was generated using two high voltage amplifier boards (OPA455 150 V amplifier from Texas Instruments) driven by an arbitrary waveform generator (AWG). The field between the two plates can be approximated as:

$$E \approx \frac{V_{plates}}{4} V_{pp}/cm$$

where  $V_{plates}$  is the peak-peak magnitude of the potential difference across the plates. The probes are securely held in the center of the two plates using a 3D printed holder.

### A. Frequency Response

The probe, with a dimension of 3 mm, operates in the quasistatic regime, as its size is significantly smaller than the wavelength of the applied 200 kHz signal, calculated as:

$$\lambda = \frac{c}{f} = 3 \times 10^8 / (200 \times 10^3) = 1500 \text{ m}$$

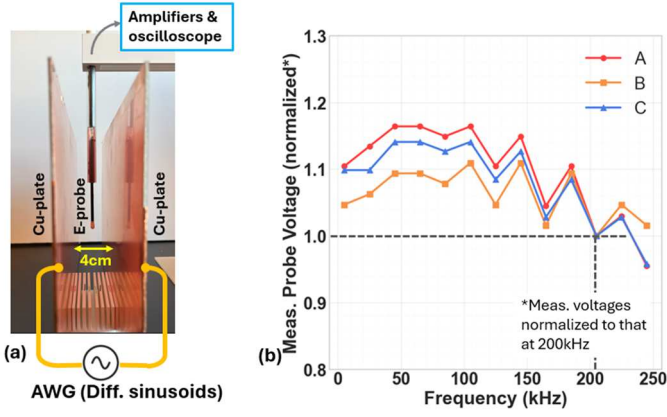


Figure 4. (a) Parallel copper plates spaced 4 cm apart with probe placed in the center. (b) Normalized measured probe voltage for frequency ranging from 5 kHz to 250 kHz

In this regime, Maxwell's equations simplify to that of electrostatics, where the electric field curl approaches zero:

$$\nabla \times \mathbf{E} = -j \frac{2\pi c}{\lambda} \mathbf{B} \rightarrow 0 \text{ as } \lambda \rightarrow \infty$$

This results in a nearly uniform electric field across the probe. The voltage induced on a short dipole in the electrostatic regime is then given by:

$$V = -\mathbf{E} \cdot d_{eff}$$

where  $d_{eff}$  is the effective length of the dipole [10]. The induced voltage is notably independent of frequency if the applied signal wavelength is much larger than the detector size.

Fig. 4(b) shows the measured voltages of 3 similarly-constructed probes on an oscilloscope, normalized to their 200 kHz values. They are relatively constant over the tested frequency range of 10 – 250 kHz, indicating that the probe will be appropriate for the proposed TTFIELD research applications. Furthermore, the device was verified that:

- variations in twisted pair cable length (and, therefore its inductance and capacitance) did not affect the frequency response, and
- varying amounts of the twisted pair cable exposed to the parallel copper plates produced no discernable output variation.

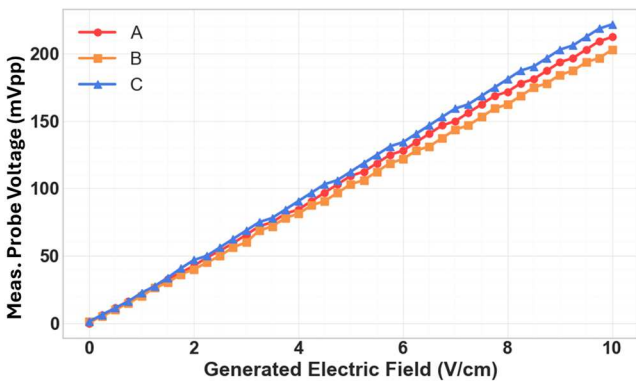


Figure 5. Amplitude response to uniform 200 kHz AEF for three probes (for fields ranging from 0.1 to 10 V/cm).

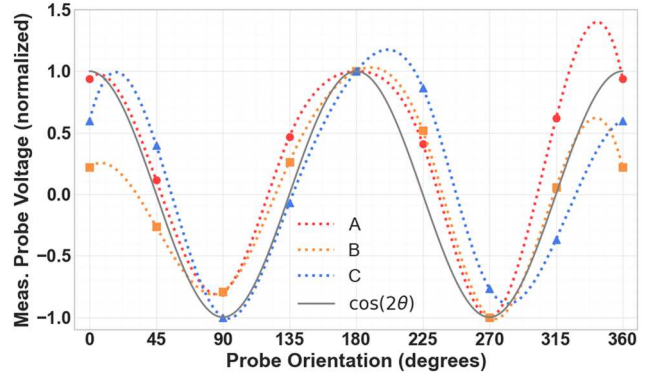


Figure 6. Normalized measured probe voltage at increments of 45° rotation (where dotted lines show the cubic spline interpolation)

### B. Calibration

Calibration is performed by placing each probe in a known electric field generated using the plates discussed earlier. Fig. 5 shows the measured probe voltage in mVpp for different applied electric fields at a constant frequency of 200 kHz. All probes show linear voltage responses over the tested AEF range of 0.1 – 10 Vpp/cm. Calibration factors are found from these linear relationships. The measured electric field is then simply given by:

$$E\text{-Field (V/cm)} = k \times \text{Meas. Probe Voltage (mVpp)} + b$$

where  $k$  is the calculated calibration factor, and  $b$  is the offset when the probe voltage is zero.

### C. Directivity

Fig. 6 plots the measured probe voltages (normalized at 180°) for three probes over the full range of orientations. The measured voltage is a maximum when the axis of the probe is parallel (180°) to the applied AEF. While the similarity to the expected sinusoidal behavior ( $\cos(2\theta)$ ) is clear, we suspect the remaining variation is a result of inconsistency in the orientation (and even tilting) of the small probes when they are fabricated.

### D. Comparison to a Commercial Probe

To illustrate the advantages of our proposed probe we compare it to a commercial stub probe (Beehive 100D EMC probe) [11]. The two probes are placed at three distinct locations in a uniform AEF. Table II shows the measured results. It is observed that the stub probe has a percentage error of 94.4 %. The "A" probe has a percentage error 18.0 % when the amplification electronics are isolated. It highlights the importance of the proper earth ground isolation.

TABLE I. COMPARISON TO COMMERCIAL PROBE

Probe Position (between 2 Cu-plates, 4cm apart)	Meas. E-field (V/cm)	
	Commercial ("Beehive") Probe	Proposed Probe (A)
"Left", 1cm*	5.01	5.90
"Center", 2cm*	0.29	5.00
"Right", 3cm*	5.02	4.60
Max. % Error	94.2%	18.0%

(\*distance from the left Cu-plate)



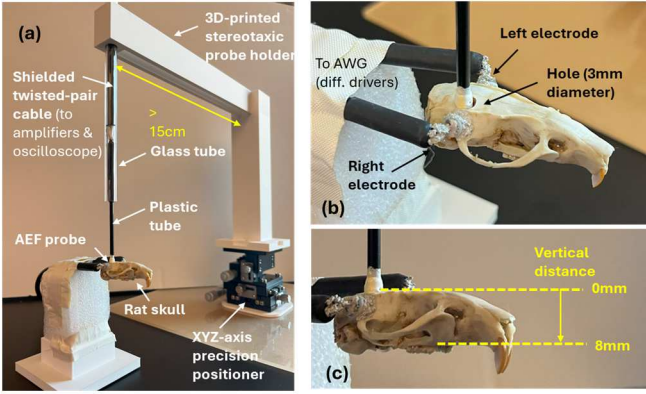


Figure 7. (a) Full experimental setup showing the probe, rat skull and XYZ-axis positioner. (b) Close up of rat skull with attached electrodes. (c) Side view indicating vertical distance

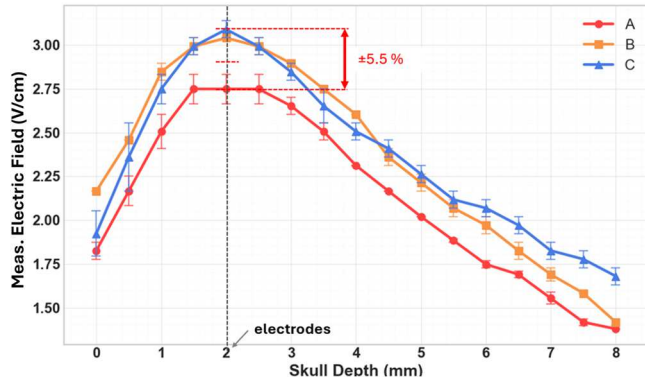


Figure 8. Measured electric field for three probes (A, B, C, each measured 3 times) at different vertical distances into the rat skull.

#### IV. ELECTRIC FIELD MEASUREMENT IN RAT SKULL

##### A. Experimental Setup

Fig. 7(a) shows the full test setup for AEF measurement inside a rat skull. A 3D printed holder is used to securely hold the probe in place above the rat skull. The holder is placed on a precision XYZ positioning stage which can be used to lower the probe into a small burr hole on top of the skull. To minimize field perturbation by external metallic components, the rat skull is placed far away from the movement stage and supported by foam. Similarly, through a long (60 cm) shielded cable connected to the probe, the amplification electronics are also placed far away. Two electrodes are connected to the skull using silver epoxy as shown in Fig. 7(b). The total vertical distance from the top of the skull to the bottom of the skull is 8 mm as shown in Fig. 7(c). The precision positioning stage allows us to precisely lower the probe into the skull in 0.5 mm increments.

##### B. Results

Fig. 8 plots the measured electric field for probes A to C as a function of the vertical distance into the skull. Very similar trends were observed. Peak AEF magnitude was measured at the 2 mm depth, which is the location of the electrodes. Consistent results were achieved over repeated (3 ×) tests, as indicated by the error bar

When comparing the measured electric field between the three constructed probes, we observe a percentage error of  $\pm 5.5\%$  at the peak response. We believe the error can be reduced by:

- Better isolation of electronics from earth ground,
- Improved mechanical positioning of the sensor, and
- Improved dipole mounting techniques for more precise orientation.

#### V. CONCLUSION

This work introduces an initial design and test of a 3 mm electric field sensor based on a dipole for low-frequency alternating electric field (AEF) measurements in preclinical applications. This probe system has the potential to outperform known methods of AEF sensing by satisfying the strict constraints these applications impose such as extremely small size with minimal perturbation of the applied field without the need for complicated fabrication methods.

#### ACKNOWLEDGEMENTS

This research was supported by Baylor Engineering and Computer Science (ECS) Dean's Development Fund. CBP is a McNair Scholar supported by the McNair Medical Institute at The Robert and Janice McNair Foundation.

#### REFERENCES

- [1] Pohling C, et al., Current status of the preclinical evaluation of alternating electric fields as a form of cancer therapy. *Bioelectrochemistry*. 2023 Feb; 149:108287.
- [2] J. Shuren, "Letter from the FDA to the FCC on Radiofrequency Exposure," April 24, 2019. [On-line]: <https://www.fda.gov/media/135022/download>
- [3] "IEEE Standard for Safety Levels with Respect to Human Exposure to Electric, Magnetic, and Electromagnetic Fields, 0 Hz to 300 GHz," in *IEEE Std C95.1-2019*, Oct. 2019.
- [4] Zheng W. et al., Principle and characteristic analysis of electric field sensor. *Proc. SPIE, 9<sup>th</sup> Int. Symp. on Sensors, Mechatronics, and Automation System (ISSMAS 2023)*, 1298113 (2024).
- [5] Pant M, and Malviya L. Design, developments, and applications of 5G Antennas: a review. *International Journal of Microwave and Wireless Technologies*. 2023;15(1): 156–182.
- [6] M. Kanda, "Standard probes for electromagnetic field measurements," in *IEEE Transactions on Antennas and Propagation*, vol. 41, no.10, pp. 1349–1364, Oct. 1993.
- [7] Miller DL. Miniature-probe measurements of electric fields induced by 60 Hz magnetic fields in rats. *Bioelectromagnetics*. 1996; 17(3):167-73.
- [8] Liu, Chengzhi et al., "A High-Performance Composite Electric Field Probe With Bandwidth 5 kHz-2 GHz of Normal and 5 kHz-500 MHz of Tangential." *IEEE Transactions on Instrumentation and Measurement* 74 (2025): 1–13.
- [9] Guanghua Li, David Pommerenke, and Jin Min. "A Low Frequency Electric Field Probe for Near-Field Measurement in EMC Applications." *IEEE International Symposium on Electromagnetic Compatibility (EMC)*. IEEE, 2017. 498–503.
- [10] D. H. Staelin, *Electromagnetics and Applications*. Cambridge, MA: Massachusetts Institute of Technology, 2011.
- [11] 100D EMC Probe [On-line]: <https://www.beehive-electronics.com/probes.html>